A Novel and High-Precision Optical Displacement Sensor

A. Rostami[a, b], M. Noshad[a], H. Hedayati[a], A. Ghanbari[b] and F. Janabi-Sharifi[b, c]

[a] Photonics and Nanocrystal Research Lab., Faculty of Electrical and Computer Engineering, University of Tabriz, Tabriz 51664, Iran

[b] Center of Excellence in Mechatronics, University of Tabriz, Tabriz 51664, Iran

[c] Department of Mechanical and Industrial Engineering, Ryerson University, Toronto, Canada M5B 2K3

Summary

In this paper, theoretical and experimental investigation of a novel compact and high-precision (0.2 nm) optical displacement sensor is presented. The sensor operation is based on optical intensity modulation due to diffraction. A circular disk, including a central transmitter and circumferential receivers (8 and 12 configurations), is considered as high precision displacement sensor. Effects of the number of receivers and the reflection coefficient of the receiver's surface on sensitivity of the proposed sensor are investigated. It is shown that with increase of the reflection coefficient of the surface, the sensitivity will increase up to five times compared with the traditional case. It is also demonstrated that there is an excellent agreement between theoretical and experimental results.

Key words:

Displacement sensor, High resolution, Fiber optic sensor, Diffractive optics, Intensity variation.

1. Introduction

High-precision distance sensors have received significant attention in the recent years with the advances in MEMS and nanotechnology. Potential applications range from industrial to medical fields and include reverse engineering, micro-assembly, and micro-surgery. In particular, many processes use distance feedback and hence, the process operation is highly affected by the precision of measurements. Despite extensive work on distance sensors, existing sensors embody certain limitations in terms of accuracy, cost, and sensitivity (Amann et al., 2001; Li, 2003).

Among different possible media for measurements, optical measurements offer significant advantages such as immunity to electromagnetic interference, large bandwidth, high precision, high sensitivity, ease of data processing, ease of communication, flexible circuits, and circuit miniaturization (Knopf, 2003; Li, 2003). Growth of interest in optical-fiber sensors has been accelerated by the recent advances in all branches of optical engineering, including opto-electronics, opto-mechatronics, and optical signal processing. In particular, there is a high demand for optical distance sensors with higher performance and smaller scale. The demand for better performance is dictated by the requirements for higher resolution and accuracy, larger measuring range, better linearity, simpler construction, and lower cost. When it comes to size, smaller sizes are highly desirable in many emerging areas such as optics, MEMS, MOEMS, electronics and biotechnology, to name a few.

Therefore, a significant attention has been devoted towards miniaturizing optical distance sensors in the last decade (Miyajima et al., 1998). This is because the size of the sensor has a strong relationship with the total size and cost of many types of industrial equipment. Additionally, reduced size of a sensor could create new applications by allowing the sensor to be embedded into small areas. Examples for emerging applications of micro-size high-precision optical distance sensors (with nanometer resolution) include micro factory automation and semiconductor manufacturing. Yet the applications are limited by the resolution of existing sensors.

Advances in the design of lasers, integrated optics, MOEMS, emitter-and-receiver electronics will all lead to design of better distance sensors with improved resolution and even further interesting developments. A dominant technology of CMOS currently allows integration of optical metrology (with photodiode, analog and digital circuits) on a single chip. One of the interesting results is development of interferometric linear encoder principle using diffraction grating (Fourment et al., 2004). The principle of using grating for displacement measurements was described in the previous work (Prelle, et al., 2002 ; Lamarque and Prelle, 2002). A few integrated single-chip systems have been also designed. For instance, a miniaturized displacement fiber optic sensor was presented by Ito et al. (2003) where the laser diode, photodiode and waveguide were integrated on a 0.8mm×0.75mm GaAs substrate. Some other earlier results include works of Ikawa et al. (1987) and Wang (1999), who reported development of an analogical fiber

Manuscript received April 5, 2007
Manuscript revised April 25, 2007

optic displacement sensor to fulfill the long-range and the nanometric resolution requirements. In previous work, amplitude-modulation-based sensors used the modulation of light power transmitted between the head of the sensor and the target surface, e.g., in (Wang, 1997). For large range cases, there are some published ideas reporting that the measured distance could be increased by making a custom prototype grating, e.g., in (Prelle, et al., 2002).
However, in the previous work, there is no investigation about effects of the surface quality of the photodiodes (as receivers of the modulated intensity) and number of photodiodes on resolution. This paper contributes by reporting an investigation on the effect of surface quality of receivers and number of photodiodes. Furthermore, based on the investigation, a methodology is proposed to extend the resolution of displacement measurement to sub-nanometer level. Our proposal is based on increasing the number of receivers that can measure the scattered light and control of the surface quality. In the proposed sensor, light is generated by laser or light emitting diode and transmitted through a bundle of fibers onto the object. The reflected light is received by another set of fibers, and is finally measured by a PIN diode (or other traditional photodiodes). We increased the number of receiving fibers and surface quality to increase the sensitivity of the sensor. This led to achieving an ultra-high resolution of about 0.2 nm in theory. After validation of the theoretical result in experiment, the slope of the transfer function can determine the resolution of the system that is shown to be 0.2 nm. Organization of the paper is as follows. In section 2, structure of the sensor is presented and operation of the sensor is mathematically explained. Simulation and experimental results are presented in section 3. Finally, the paper is concluded in section 4.

2. High Resolution Sensor Operation Principle

The usual applications of a displacement fiber optic sensor have already been described (Kissinger, 1967; Alayli et al., 1998; Gir˜ao et al., 2001). The configuration of the proposed displacement sensor is illustrated in Fig. 1. In this analysis, we assume that the surface of a target object to be quasi-planar, i.e., can be approximated by a collection of planes. This assumption is valid for measurement of non-planar objects in close range. As it is shown in Fig. 1, the emission fiber placed in the center emits light at a given wavelength. The reflected light by the object is injected into the receiver fibers placed around the emission fiber and guided to a PIN or other photodiodes. The amount of the reflected light is a function of the distance between the sensor head and the object.

In this work the following two structures for the head of the proposed sensor are used which are illustrated in Fig. 2. In Fig. 2.a, there are 12 receiver fibers and one transmitter fiber, where in Fig. 2.b, there are 8 receiver and one transmitter fibers respectively. In this structure, we have used single mode optical fiber (non-zero dispersion shifted fiber NZDSF SM 16) including 16 fibers. One of the fibers is used for transmitter and the rest (8 or 12 depending on the configuration) were utilized for receivers. The infrared transmitter and receivers of Siemens unit-622 type operating at 1550 nm have been used.

To find the received power by the fibers, one needs to find the function of the emitting light intensity. One can assume the emitting fiber as a circular aperture and use Fraunhofer diffraction for obtaining the distribution function I as follows. It should mention that in the proposed system high resolution displacement is obtained in the range of about 150-200 mm. Therefore, far field approximation can be used. That is

$$I = 4\pi^2 C^2 a^4 \left(\frac{J_1(kau)}{kau} \right)^2, \quad k = \frac{2\pi}{\lambda}, \quad u = \frac{r}{x}, \qquad (1)$$

where C, a, λ, x, and r are corresponds to the emitted power per unit area, the diameter of the emitting fiber, wavelength, the distance between transmitter and the flat object, and image size on object, respectively, as shown in Fig. 3. Also, J_1 is the Bessel function of the first order and first kind. It is worthy of mentioning that in all of simulation results, Eq. (1) is used extensively.
For the proposed sensor typical response of simulation is shown in Fig. 4. In Fig. 4.a the received intensity versus distance is illustrated. In Fig. 4.b, the received intensity for below 400 mm is shown. The linear range of operation is demonstrated in Fig. 4. As it is shown in Fig. 4, for 208–256 mm, the received intensity (56.55–90.48 mW) is linearly related to displacement. These figures are related to the first disk (Fig. 2.a) of the receiver head (with 12 receivers). Slope (Slope of received power-distance curve) of the linear zone determines the resolution of the sensor. The sensor resolution can be defined as follows.

$$\text{Resolution} = {}^{\Delta X}\Big|_{\Delta P:\ \text{minimum detectable (received) power}}$$

that can be determined easily from obtained transfer function.
The similar case for the second type of head of the sensor (8 receivers) is illustrated in the Fig. 5. In Fig. 5.a, the received intensity versus long range displacement is illustrated. Also, the received intensity for displacement below 500 mm is illustrated in Fig. 5.b. It is shown that for displacement range of 160–192 mm, there is a linear

relationship between received intensity (26.1–49.88 mW) and displacement.

For extraction of the aforementioned figures, output current of all of photodiodes are summed up and then is amplified by low noise operational amplifier in a form of instrumentation configuration. Therefore, output signal of the designed circuit is related by a constant (gain) to the received intensity. The electronic circuits used in the sensor are conventional and can be found in any electronic text books. There are four photodiodes around the transmitter, arranged in parallel. The electric currents generated in these photodiode are summed and passed through a resistor in the emitter of the phototransistors. Then the generated voltage is passed through an instrumentation amplifier designed using three op-amps or complete instrument amplifier chip. Finally, the output of this block is amplified output voltage of measured signal.

According to basic circuit theory, the following relations hold for output signal corresponding to displacement.

$$V_O = 1.2^{K\Omega} \sum_{i=1}^{8} I_i \quad , \ (2)$$

where I_i is current component created corresponding to received power in that position. The upper limit of sum in Eq. 2 will be 12 in the case of 12 receivers. The relationship between diffracted light for generated current is given in Eq. 3. In linear range of operation, the generated current corresponds to the received power as follows.

$$I_i = \xi_i P_i \quad , \ (3)$$

where ξ_i and are slope of transfer function and incident power on i^{th} receiver P_i , respectively. In terms of generated current, with given power on receiver, the generated current can be measured and the constant relating diffracted power and generated current is determined.

The generated voltage in the sensor is then applied to the conditioner circuit. The total output voltage after instrumentation amplifier is given as follows.

$$V_{O_{Total}} = \left[-\frac{R_3}{R_2}\left(1 + \frac{R_1 + R_2}{R_G}\right) \right] \left[1.2^{K\Omega} \sum_{i=1}^{4} (\xi_i \zeta_{(x-P)_i}) \right] x \quad , \ (4)$$

where *x* is the distance between sensor and object, ξ_i and $\xi_{(x-P)_i}$ are linear slope of current versus incident power, and linear slope of displacement and received power, associated with the i[th] receiver, respectively. For similar receivers, the constants do not vary. R_i is the amplifier parameter. For derivation of Eq. 4, first bracket is the transfer function of the proposed instrument amplifier (that can be derived based on basic electronic circuit theory) and the second part is a relation between diffracted light and generated voltage (that can be described with linear relation).

From illustrated curves, one can conclude that 48 and 32 mm linear ranges of operation can be obtained. Therefore, it is observed that with increase of the number of receivers, linear range of operation and resolution are increased. In addition, the received power in the first case is better than the second case.

3. Simulation and Experimental Results

In this section, the simulation and experimental results are presented, and discussions are made. The purpose of the simulations and experiments was to study the effect of the number of receivers and the surface quality on the sensor performance, and also to evaluate the degree of agreement between simulation results (based on the theoretical formulation) and the experimental results.

Our setup included an infrared transmitter, some infrared receivers, and optical encoder of a standard CNC machine (Emcotronic TM02) that was used for displacement calibration. For input source, we used infrared transmitter with 148 mW power, 8 um diameter related fiber and 1550 nm wave length. For receivers infrared photodiodes with same characteristics as transmitter only with 14 um diameter were used. Electronic conditioner circuit accompanying the photodiodes converted the received power to electrical current. Finally, a low noise operational amplifier summed the output current of the photodiodes and generated an output signal corresponding to the diffracted power from the object. For experimental measurements, we used CNC machine (Emcotronic TM02) for setting displacement with 10 mm resolution (Fig. 6). In the sensor analysis, the incident light power from the transmitter was assumed be 148 mW, which was kept the same throughout all simulations and experiments.

Effect of the nonzero reflection coefficient of the surface of the proposed head of displacement sensor on the received power, linear range of operation, and device sensitivity are illustrated in Fig. 7. It was shown that with increase of the reflection coefficient, the received power raises and sensitivity is increased. Also, in Fig. 7, the cases with and without reflection are compared together. Obviously the existence of the reflection coefficient considerably increases the device performance. These properties can be explained based on the fact that the reflected light from the object is reflected from surface of

the head and impact on object and propagated backward and finally received by photodiodes.

In the following, we present a simulation curve for the case of zero reflection. Also, the measured data for this situation is illustrated (Fig. 8). The simulation and experimental curves in Fig. 8 considerably coincide, suggesting that the proposed sensor can be used in practice with estimated properties in the simulation results.

In the second experiment, we considered a nonzero reflection for the surface of the head of the proposed sensor. In this case the reflection coefficient of 85% is considered. Fig. 9 includes the theoretical and experimental results for this case. In addition, in this case, an excellent matching between experimental and the theoretical (simulation) results is observed.

The results also show that the proposed device would exhibit sub-nanometer resolution that could highly impact and potentially benefit many applications requiring high-precision displacement sensors. First we validated the proposed theoretical idea in experiment and then according to the obtained transfer function, high resolution is predicted and it is shown that the proposed idea has capability to increase resolution of the optical fiber displacement sensor.

4. Conclusion

In this paper, a high-resolution fiber optics displacement sensor was proposed. Within the linear range of sensor operation, our proposed sensor demonstrated sensitivity as high as 0.2 nm. It was shown that with increase of the surface (of the head) reflection coefficient, the linear range of operation, sensitivity and the received power are increased. Therefore, the proposed idea illustrates a new insight into design of high resolution displacement measurement tools. Using the proposed method in this paper, we will keep our effort to extend and develop the sensor, and to achieve even better sub-nanometer resolution. Our future work will also include investigation on displacement sensor with tilted receivers for improving the resolution. This is motivated by the fact that there is high power of diffracted intensity that propagates with off normal angle(s). Arranging receivers to be normal to this diffracted surface, a further improvement is plausible.

References

[1] Alayli Y., Wang D., Bonis M. 1998. Optical fiber profilometer with submicronic accuracy. Proc. SPIE 3509:84–87.

[2] Amann, M.-C., T. Bosch, M. Lescure, R. Myllylä, and M. Rioux. 2001. Laser ranging: a critical review of usual techniques for distance measurement. Opt. Eng. 40(1):10-19.

[3] Fourment S., Arguel P., Noullet J.-L., Lozes F., Bonnefont S., Sarrabayrouse G., Jourlin Y., Jay J., Parriaux O. 2004. A silicon integrated optoelectro- mechanical displacement sensor. Sens. Actuators A 294: 300-110.

[4] Gir˜ao P. M. B. S., Postolache O. A., Faria J. A. B., Pereira J. M. C. D. 2001. An overview and a contribution to the optical measurement of linear displacement. IEEE Sens. J. 1(4): 322–331.

[5] Ikawa N., Shimada S., Morooka H. 1987. Photoelectronic displacement sensor with nanometre resolution, Precision. Eng. 9(2): 79–82.

[6] Ito T., Sawada R., Higurashi E. 2003. Integrated micro-displacement sensors that uses beam divergence,'' J. Micromechan. Microeng. 13: 942–947.

[7] Kissinger C. 1967. Fibre optic displacement measuring apparatus. US Patent 3,940,608.

[8] Knopf, G.K. 2003. Opto-mechatonic products and processes: design considerations. in Opto-Mechatronic Systems Handbook, Edited by H. Cho, CRC Press, Boca Raton, FL.

[9] Lamarque F., and Prelle C. 2002. Analogic fiber optic position sensor with nanometric resolution 2002. Proceedings of the IEEE Sensors, Orlando, USA, June 926:930.

[10] Lee, B. 2003. Review of the present status of optical fiber sensors. Optical Fiber Technology 9(2): 57-79.

[11] Miyajima, H., E. Yamamoto, K. Yanagisawa. 1998. Optical micor encoder with sub-micron resolution using VCSEL. J. Sensors and Actuators A 71:213-218.

[12] Prelle C., Lamarque F., Mazeran P.-E. 2002. A new method for high resolution position measurement on long range. J. Eur. Syst. Autom. 36(9): 1295–1307.

[13] Prelle, C., Lamarque, F., and Revel, P. 2006. Reflective optical sensor for long-range and high-resolution displacements. Sens. Actuators A 127:139–146.

[14] Wang D., Alayli Y., Bonis M. 1997. Design and modeling of a fiber optic displacement sensor with nanometer resolution. in Proceedings of the Ninth IPES Braunschweig-PTB, 1:90-92.

[15] Wang D. 1999. Conception et réalisation d'un minicapteur de déplacement a fibres optiques de résolution nanométrique. Ph.D. Dissertation, Univ. Tech. Compiègne.

Appendix

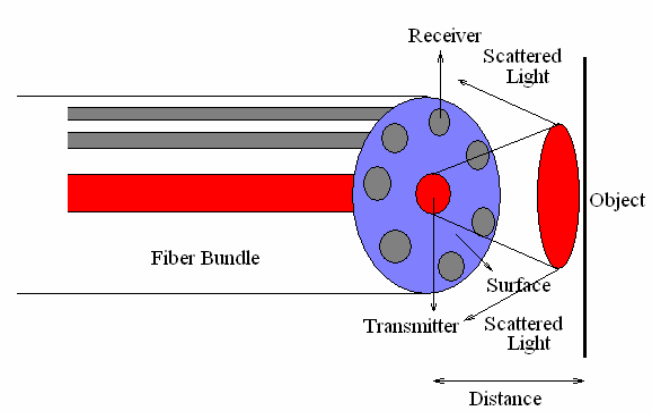

Figure 1. Schematic diagram of Fiber optic displacement sensor.

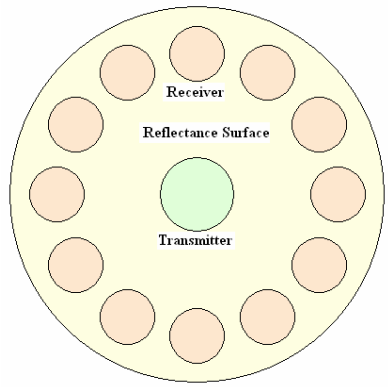

(a)

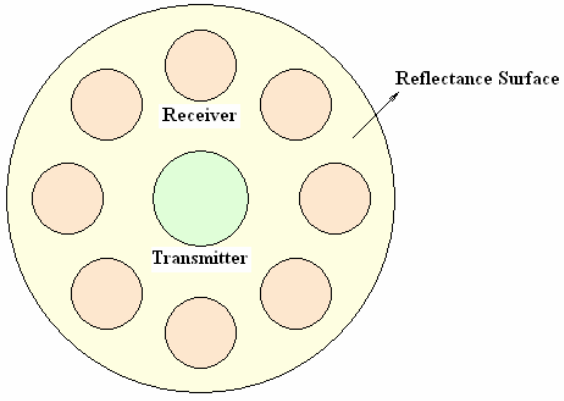

(b)

Figure 2. Two structures for the head of the proposed sensor using single mode optical fiber. (a) Twelve receiver fibers and one transmitter fiber. (b) Eight receiver fibers and one transmitter fiber. The used fiber set for experiments was non-zero dispersion shifted fiber NZDSF SM 16, where 1 fiber was used for transmitter and the rest (8 in configuration a and 12 in configuration b) were used for receivers. The infrared transmitter and receivers were Siemens unit-622 operating at 1550 nm.

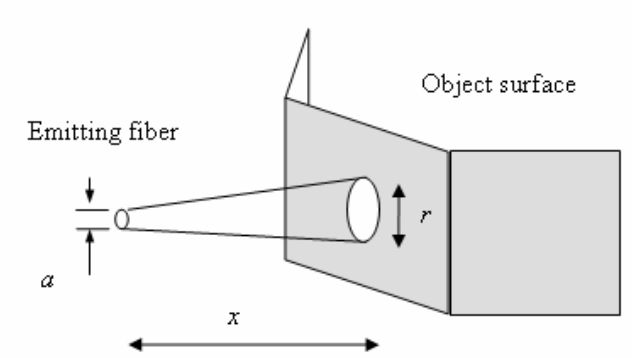

Figure 3. Schematics of diffracted light parameters on a surface approximated by planes. *x* indicates the distance between a transmitter and object.

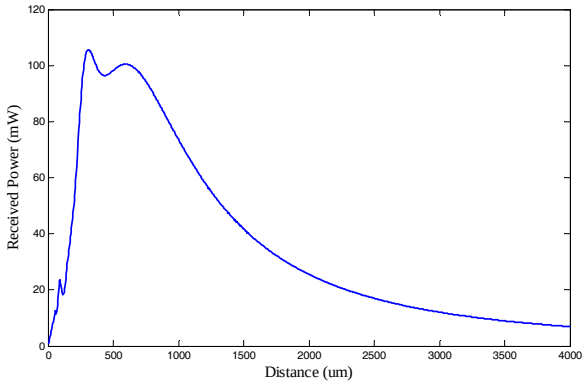

(a)

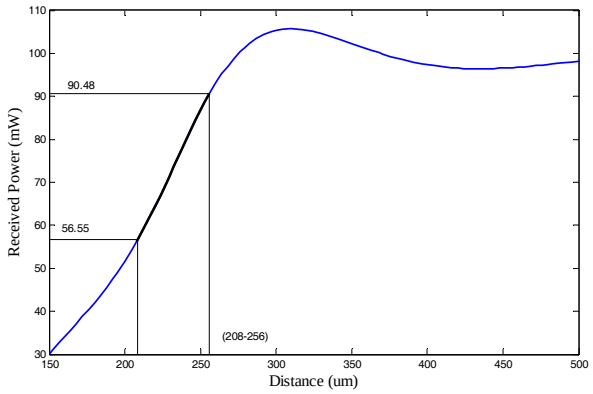

(b)

Figure 4. Typical response of the proposed sensor (a) normal view and (b) enlarged view for the linear zone, related to the first case in Fig. 2.

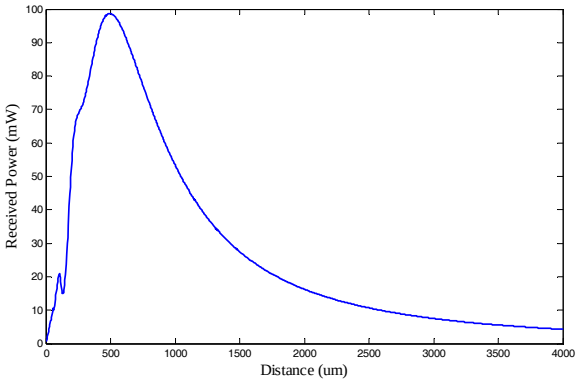

(a)

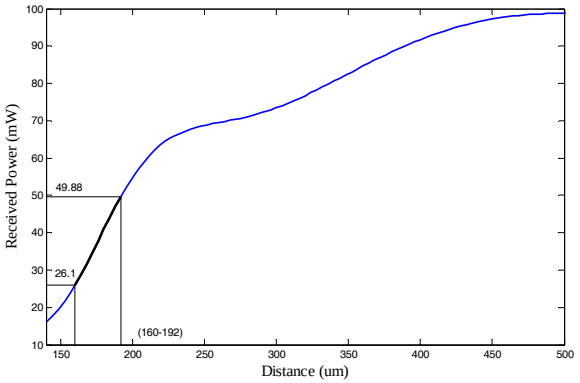

(b)

Figure 5. Typical response of the proposed sensor (a) normal view and (b) enlarged view for the linear zone, related to the second case in Fig. 2.

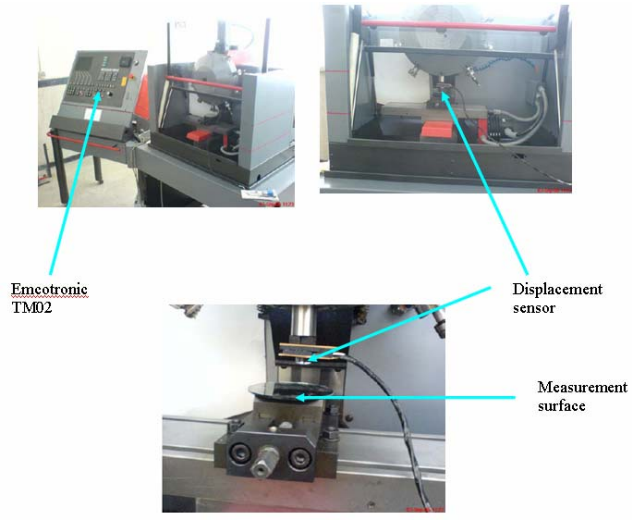

Figure 6. Experimental setup for evaluating of the proposed sensor, with different views of the setup.

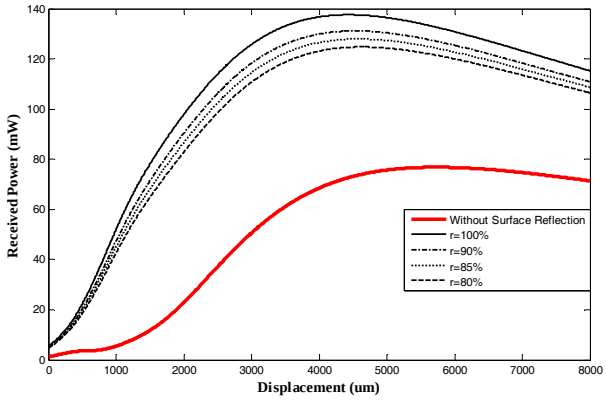

Figure 7. Received power vs. displacement with reflectance of the surface as a parameter.

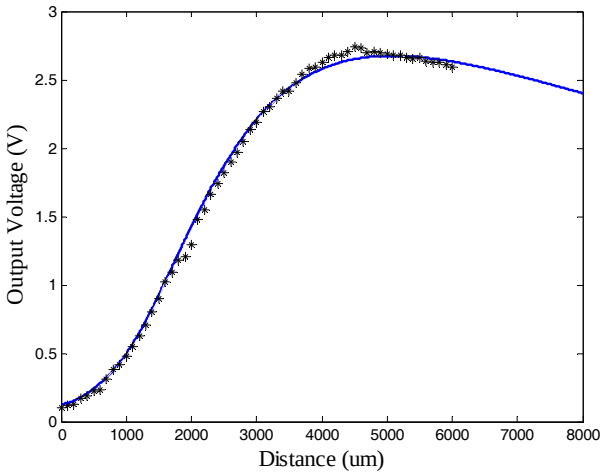

Figure 8. Output voltage of the photo detectors vs. displacement without reflectance of the surface (solid line) and experimental data (star).

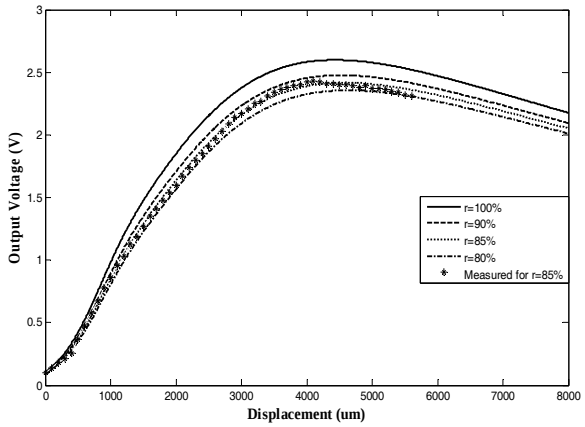

Figure 9. Output voltage of the photo detectors vs. displacement with reflectance of the surface (solid lines) and experimental data corresponds to the reflection coefficient of 85% (star).